Medical Oncology (2024) 41:49
https://doi.org/10.1007/s12032-023-02279-0

ORIGINAL PAPER

Combination of Resveratrol and PARP inhibitor Olaparib efficiently deregulates homologous recombination repair pathway in breast cancer cells through inhibition of TIP60-mediated chromatin relaxation

Saptarshi Sinha[1] · Subarno Paul[1] · Sushree Subhadra Acharya[1] · Chinmay Das[1] · Somya Ranjan Dash[1] · Subhasmita Bhal[1] · Rajalaxmi Pradhan[1] · Biswajit Das[1] · Chanakya Nath Kundu[1]

Received: 16 October 2023 / Accepted: 30 November 2023

Abstract

Recently, we reported that a combination of a natural, bioactive compound Resveratrol (RES) and a PARP inhibitor Olaparib (OLA) deregulated the homologous recombination (HR) pathway, and enhanced apoptosis in BRCA1-wild-type, HR-proficient breast cancer cells. Upon DNA damage, chromatin relaxation takes place, which allows the DNA repair proteins to access the DNA lesion. But whether chromatin remodeling has any role in RES + OLA-mediated HR inhibition is not known. By using in vitro and ex vivo model systems of breast cancer, we have investigated whether RES + OLA inhibits chromatin relaxation and thereby blocks the HR pathway. It was found that RES + OLA inhibited PARP1 activity, terminated PARP1-BRCA1 interaction, and deregulated the HR pathway only in the chromatin fraction of MCF-7 cells. DR-GFP reporter plasmid-based HR assay demonstrated marked reduction in HR efficiency in I-SceI endonuclease-transfected cells treated with OLA. RES + OLA efficiently trapped PARP1 at the DNA damage site in the chromatin of MCF-7 cells. Unaltered expressions of HR proteins were found in the chromatin of PARP1-silenced MCF-7 cells, which confirmed that RES + OLA-mediated DNA damage response was PARP1-dependent. Histone Acetyltransferase (HAT) activity and histone H4 acetylation assays showed reduction in HAT activity and H4 acetylation in RES + OLA-treated chromatin fraction of cells. Western blot analysis showed that the HAT enzyme TIP60, P400 and acetylated H4 were downregulated after RES + OLA exposure. In the co-immunoprecipitation assay, it was observed that RES + OLA caused abolition of PARP1-TIP60-BRCA1 interaction, which suggested the PARP1-dependent TIP60-BRCA1 association. Unaltered expressions of PAR, BRCA1, P400, and acetylated H4 in the chromatin of TIP60-silenced MCF-7 cells further confirmed the role of TIP60 in PARP1-mediated HR activation in the chromatin. Similar results were obtained in ex vivo patient-derived primary breast cancer cells. Thus, the present study revealed that RES + OLA treatment inhibited PARP1 activity in the chromatin, and blocked TIP60-mediated chromatin relaxation, which, in turn, affected PARP1-dependent TIP60-BRCA1 association, resulting in deregulation of HR pathway in breast cancer cells.

✉ Chanakya Nath Kundu
cnkundu@kiitbiotech.ac.in

[1] Cancer Biology Division, KIIT School of Biotechnology, Kalinga Institute of Industrial Technology (KIIT), Deemed to be University, Campus-11, Patia, Bhubaneswar, Odisha 751024, India

Published online: 06 January 2024

Graphical abstract

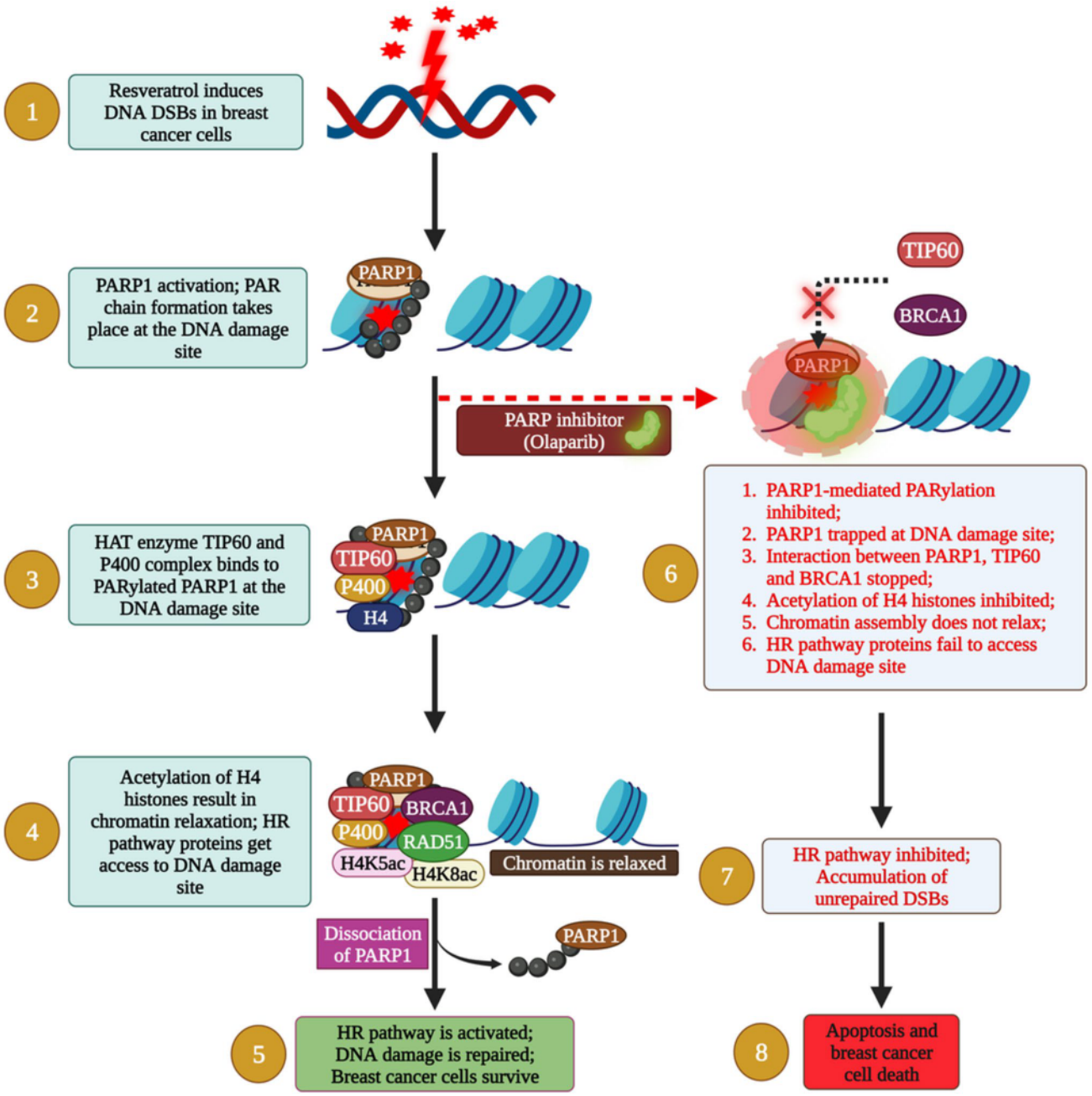

Keywords Breast cancer · Resveratrol · Olaparib · Chromatin remodeling · TIP60 · Homologous recombination repair

Introduction

Breast cancer ranks first in terms of global incidence of cancer and is the most prevalent cancer in women worldwide [1]. While treatments like radiotherapy, chemotherapy, and hormone therapy exist, development of therapeutic resistance and multiple drawbacks like high cytotoxicity and low efficacy persist [2]. Hence, urgent development of novel anticancer agents is crucial to combat this disease and improve treatment outcomes.

Poly (ADP-Ribose) polymerases (PARPs) are a group of enzymatic proteins, which are known to play important roles in multiple cellular processes, such as DNA damage and repair. Inhibition of PARP proteins causes inactivation

of DNA repair pathways, resulting in accumulation of DNA damage in the cells [3]. Under BRCA1-mutated, homologous recombination (HR)-deficient conditions, PARP inhibition leads to development of synthetic lethality in cancer cells [4]. Presently, several FDA-approved PARP inhibitors (Olaparib, Rucaparib, Niraparib, and Talazoparib) are being used for the treatment of BRCA1-mutated, HR-deficient cancers [5]. Olaparib (OLA; AZD2281), the first FDA-approved PARP inhibitor, is used for the treatment of HR-deficient, BRCA1-mutated metastatic breast cancer [6]. But, mutations in BRCA1/2 genes occur in only around 5% of all breast cancer cases [7]. Hence, the PARP inhibitors are presently being investigated for the treatment of BRCA1-wild type, HR-proficient breast cancer, in combination with other anticancer agents.

In our recently published article [8], we have reported that Olaparib (OLA), an FDA-approved PARP inhibitor, enhanced the DNA damaging potentiality of a natural, bioactive compound Resveratrol (RES) via catalytic inhibition and trapping of PARP-1 at the DNA double-stranded break (DSB) site in the BRCA1-wild type, HR-proficient breast cancer cells. RES + OLA combination treatment inhibited PARP-1-mediated PARylation and caused termination of PARP1-BRCA1 interaction, resulting in deregulation of the homologous recombination (HR) repair pathway, followed by accumulation of DSBs, induction of apoptosis and breast cancer cell death [8]. Here, it is important to understand that when a cell suffers a DNA damage, the DNA lesion site is located deep inside the dense, and highly condensed chromatin network. Then, PARP1, which is activated upon DNA damage, catalyzes PARylation of chromatin-associated proteins (like histones) and PARP1 itself (auto-PARylation). This results in histone eviction from DNA, which allows the chromatin remodeling enzymes to relax the chromatin network. When the chromatin structure is relaxed, the DNA repair proteins get access to the DNA damage site and repair it [3, 9]. Hence, if the PARP-1 enzymatic activity can be inhibited by using a PARP inhibitor, then it may lead to inhibition of the chromatin remodeling events and simultaneously block the DNA repair pathways, resulting in the accumulation of DNA damage in cancer cells. But it has been previously observed that the PARP inhibitors exhibit their optimal functioning only after induction of DNA damage by another chemotherapeutic agent [10]. Multiple studies have shown that PARP inhibitors sensitize the cancer cells to different DNA-damaging agents [11, 12]. However, it remains to be established whether RES + OLA combination can inhibit relaxation of the chromatin structure and block the HR pathway proteins from accessing the DNA damage site.

RES has been found to cause DNA damage in the form of double-strand breaks (DSBs) in different cancer cell lines [13]. In response to DSBs, histone H4 is rapidly acetylated on the nucleosomes at the DNA damage site. H4 hyperacetylation is catalyzed by the histone acetyltransferase (HAT) TIP60, which functions as a subunit of the human NuA4 (hNuA4) remodeling complex in DSB repair. Previous studies have shown that inactivation of TIP60 inhibited H4 acetylation, which increased sensitivity of cells to DNA damage [14]. Another study recently reported that PARP-1 is a component of TIP60 HAT complex and their interaction increases after induction of DNA damage [15]. Apart from TIP60, the hNuA4 complex also contains three other subunits possessing catalytic activity: P400 motor ATPase, and Ruvbl1 and Ruvbl2 helicase-like proteins. P400 induces replacement of histone H2A with the histone variant H2A.Z, which results in destabilization of the nucleosomes around the DSB site. This, in turn, facilitates the acetylation of histone H4 by TIP60 and its cofactor TRRAP (Transformation/Transcription Domain-Associated Protein). H4 hyperacetylation promotes relaxation of the chromatin structure, which allows BRCA1 and other HR pathway proteins to access the DSB site [16]. A recent study has shown that P400 is important for HR-dependent processes, including binding of RAD51 to the DSB and its absence resulted in a defective DSB repair [17].

Although we have previously reported that OLA significantly enhanced the apoptotic potentiality of RES in breast cancer cells, the detailed mechanism of RES + OLA combination treatment in the deregulation of chromatin remodeling after induction of DSBs is still unknown. Hence, in the present study, we have attempted to elucidate the action of RES + OLA in modulation of chromatin structure assembly in in vitro and ex vivo pre-clinical model systems of breast cancer. We have shown that this combination treatment triggered breast cancer cell death by deregulating the HR pathway through inhibition of TIP60-mediated chromatin relaxation.

Materials and methods

Cell culture and reagents

MCF-7 breast cancer cells (ATCC® HTB-22™) were cultured in DMEM culture media, containing 10% FBS, 1.5 mM L-glutamine and 1% antibiotic (100 U/ml of penicillin, 10 mg/ml of streptomycin) and maintained in a humidified atmosphere of 5% CO_2 at 37 °C. These MCF-7 cells have been used by our group previously [8] and were tested free from mycoplasma contamination. The patient-derived primary breast cancer cells were cultured and grown according to the method described earlier [8]. All the cell culture reagents were purchased from Himedia, India. The drugs RES and OLA were purchased from Sigma-Aldrich (St Louis, MO, USA) and AdooQ BioScience LLC, USA, respectively.

The antibodies anti-MRE11 (#4895), anti-BRCA1 (#9010), anti-RPA70 (#2267), anti-BRCA2 (#10741), anti-XRCC1 (#2735), anti-rabbit IgG-HRP (#7074), and anti-mouse IgG-HRP (#7076) antibodies were purchased from Cell Signaling Technology, MA, USA. Anti-RAD51 (ab63801), anti-DNA PKcs (ab70250) antibodies were purchased from Abcam, MA, USA. Anti-TIP60 (GTX112198), anti-P400 (GTX116689), anti-H4K5ac (GTX88005), anti-H4K8ac (GTX59547), anti-Histone H4 (GTX129561), and anti-Lamin B1 (GTX103292) antibodies were purchased from GeneTex, CA, USA. Anti-PAR (4335- MC-100) antibody was purchased from Trevigen, Gaithersburg, MD. Anti-rabbit (TRITC conjugate) (E-AB-1053) and anti-rabbit (FITC conjugate) (E-AB-1014) antibodies were purchased from Elabscience, USA.

Human-specific BRCA1-siRNA (#sc-29219) and control (scrambled) siRNA (#sc-37007) were purchased from Santa Cruz Biotechnology® (Santa Cruz, CA, USA). Human-specific TIP60 (KAT5)-siRNA (Assay ID 110507) and PARP1-siRNA (Assay ID 10038) were purchased from ThermoFisher Scientific India. DR-GFP (#26475) and CBASceI (#26477) plasmids were purchased from Addgene®, MA, USA.

Treatment with drugs

As per our previous study [8], the MCF-7 breast cancer cells were treated with RES (25 µM) and OLA (4 nM) for 30 h in individual treatments. In case of combination treatment, the cells were pre-exposed to 10 µM of RES for 6 h, followed by treatment with OLA (4 nM) for 24 h. The patient-derived primary breast cancer cells were also treated with similar concentrations of RES and OLA in both individual and combination treatments.

Isolation of nuclear and chromatin fractions

RES and OLA treated cell lysates were fractionated into nuclear and chromatin fractions to determine in which compartment PARP inhibition and HR pathway blockade occurred [18]. In brief, approximately 1×10^6 cells were grown in a 6-well plate to 80–90% confluency and treated with RES, OLA, and their combination for the stipulated time period. Then, isolation of the nuclear fractions was performed using NE-PER kit (PIERCE Biotechnology, Cat#78,833), while extraction of the chromatin fractions was done by using chromatin extraction buffer (50 mM HEPES, 100 mM KCl, 0.25% Triton-X-100, 10 mM NaF, 2.5 mM $MgCl_2$, 1 mM DDT, 1 mM $CaCl_2$ in distilled water). These isolated nuclear and chromatin fractions were used in the subsequent experiments.

Western blot analysis

Western blotting was performed according to our laboratory protocol [19]. Briefly, 1×10^6 cells were cultured in a culture plate and allowed to attain 80–90% confluency before RES, OLA, and RES + OLA treatments. Then, after harvesting the drug-treated cells and lysing them with modified RIPA lysis buffer, the cellular lysates were used for western blot analysis. 80 µg protein was separated by SDS-polyacrylamide gel electrophoresis (SDS-PAGE), followed by transferring of the proteins onto nitrocellulose membrane. Then, the membrane was first blocked with 10% skim milk in 1X TBST for 1 h, and incubated with specific primary and secondary antibodies (1:1000 dilutions) according to the manufacturer's protocol. The membrane was then washed with 1X TBST and processed for densitometric analysis.

Immunoprecipitation assay

Immunoprecipitation assay was performed as described earlier to measure the interactions between selected HR cascade proteins with PARP-1 and TIP60 [20]. Briefly, cells were treated with the above drugs and nuclear and chromatin fractions were isolated as mentioned above. Then, BSA-blocked protein A-Sepharose 4B was incubated with anti-PARP-1 and anti-TIP60 antibodies or IgG rabbit (for control) for 6 h at 4 °C. Approximately, 150 µg of nuclear and chromatin fractions were incubated by rocking at 4 °C with the beads overnight. Then, the beads were washed twice with 1X PBS, suspended in SDS-sample loading buffer and the soluble proteins were separated by SDS-PAGE, transferred onto a PVDF membrane, and probed with each antibody according to the manufacturer's protocol.

Determination of PARylation of PARP-1 in vitro

PARP1-mediated PARylation was checked in the cells before and after drug treatments according to our laboratory protocol [18]. Briefly, MCF-7 cells were grown in culture plates till 70–80% confluency. After drug treatments, the cells were collected and the nuclear lysates were prepared following our protocol. The nuclear lysates were immunoprecipitated with either IgG (negative control) or anti-PARP-1 and kept for incubation in PARylation reaction buffer (50 mM Tris HCl (pH 7.8), 25mM $MgCl_2$, 1mM DTT, 100 µM NAD^+, and protease inhibitors) at 37 °C for 30 min. The PAR chain forming reaction was stopped by adding SDS-PAGE sample loading buffer. Protein separation was done by SDS-PAGE, followed by nitrocellulose membrane transfer to carry out western blotting. Then, the membrane was incubated with

specific antibodies using the manufacturer's protocol and processed for densitometric analysis.

Immunocytochemical staining for BRCA1, TIP60, and H4K5Ac expressions

Immunofluorescence assays were performed according to our laboratory protocol [8] to observe the changes in the expressions of BRCA1, TIP60, and acetylated histone H4 (H4K5Ac) before and after individual and combination treatments of RES and OLA. Briefly, after growing MCF7 cells on coverslips in 24-well tissue culture plates, they were exposed to individual and combination treatments of RES and OLA. After drug treatments, the cells were first washed with 1X PBS, followed by methanol:acetone (1:1) fixation at -20 °C for 15 min. After washing the cells again with 1X PBS, they were incubated with primary anti-BRCA1 and anti-TIP60 antibodies in one experiment and anti-H4K5Ac (1:500 dilutions in 1X PBS) antibody in another separate experiment at 4 °C. Next day, after washing off the unbound antibodies with 1X PBS, the cells were incubated with secondary anti-rabbit IgG conjugated to FITC (for anti-TIP60 and anti-H4K5Ac) and TRITC (for anti-BRCA1) (1:750 dilution in 1X PBS) at room temperature for 2–3 h. After incubation, the cells were washed with 1X PBS, followed by DAPI nuclear staining. Then the cells were observed under an inverted fluorescence microscope (Nikon, Japan) at 20X magnification to observe the changes in the protein expressions before and after drug treatments.

DR-GFP reporter plasmid-based homologous recombination (HR) efficiency assay

The effect of PARP inhibitor (OLA) on the HR pathway activity in breast cancer cells was analyzed by performing DR-GFP reporter plasmid-based HR efficiency assay [8]. Two plasmids, the HR reporter plasmid (pDR-GFP) and I-SceI endonuclease encoding plasmid (pCBASceI), were used in this assay. First, the cells were grown in a 6-well plate overnight. Then the plasmids were transfected into cells with the help of Lipofectamine-2000® transfection reagent (Thermo-Fischer Scientific, MA, USA) by following manufacturer's protocol. Next, after treating the pCBASceI-transfected cells with OLA for 24 h, the cells were collected, resuspended in ice-cold PBS, and detection of GFP-positive cell population was performed using a FACS CANTO II flow cytometer (Becton-Dickinson, CA).

PARP-DNA (fluorescence polarization) trapping assay

The fluorescence polarization method of quantitative PARP-DNA trapping assay was performed with the PARP-trap™ Assay kit (cat# 80,584; BPS Bioscience, San Diego, CA) by following the principle and protocol described earlier [8]. Briefly, cells were grown in 60 mm discs for 24 h till 60–70% confluency. Then the cells were treated with RES, OLA, and their combination for the stipulated time periods. The cells were harvested, and cell lysates were prepared. Equal amounts of fluorescent labelled nicked DNA, NAD^+, and PARPtrap™ assay buffer were added to 50 µg of lysates in a 96-well plate. Then, 10 µM PARPi (OLA) was added and incubated for 30 min. Fluorescence polarization was measured in a microplate reader with excitation wavelength range of 475–495 nm and emission wavelength range of 518–538 nm (microtiter-plate reader, Eppendorf).

Knockdown of BRCA1 and TIP60 in MCF-7 cells

BRCA1 and TIP60 expressions were knocked down in MCF-7 cells using a siRNA transfection protocol described earlier [21]. In brief, equal amounts (0.25 µg) of BRCA1 or TIP60 siRNA and scrambled siRNA (control) were transfected into MCF-7 cells with the help of Lipofectamine-2000® transfection reagent (Thermo-Fischer Scientific, MA, USA). Western blot analysis was performed to validate the BRCA1 and TIP60 knockdowns in MCF-7 cells.

Histone acetyltransferase (HAT) activity assay

HAT enzymatic activity was measured using a HAT Activity Colorimetric Assay Kit (ab65352, Abcam, Cambridge, UK) according to the manufacturer's protocol [22]. Briefly, 50 µg of nuclear extracts from untreated and RES, OLA, and RES + OLA treated MCF-7 cells were incubated with HAT substrate I, HAT substrate II, and NADH-generating enzyme in HAT assay buffer for up to 4 h at 37 °C. A microplate reader (Epoch, BioTek Instruments, Winooski, VT, USA) was used to measure the absorbance at 440 nm.

Histone H4 total acetylation colorimetric assay

Detection and quantification of acetylated histone H4 was performed using a Histone H4 Total Acetylation Detection Fast Kit (Colorimetric) (ab115125, Abcam, Cambridge, UK) according to the manufacturer's protocol [23]. Briefly, untreated and RES, OLA, and RES + OLA treated MCF-7 cells were harvested and centrifuged at 1000 rpm for 5 min at 4 °C. Then the cell pellets were resuspended in TEB buffer at 10^7 cells/mL and lysed on ice for 10 min with gentle stirring. After centrifugation at 10,000 rpm for 1 min at 4 °C, the supernatants were discarded and the pellets were resuspended in extraction buffer (0.5 N HCl + 10% glycerol). After 30 min incubation on ice, the samples are centrifuged at 10,000 rpm for 5 min at 4 °C. Then acetone is added to the supernatants and incubated at − 20 °C overnight. Following

centrifugation at 12,000 rpm for 5 min at 4 °C, the pellets are air-dried and then dissolved in distilled water. These histone extracts were quantified and used for the H4 acetylation assay. In the assay, the acetylated histone H4 present in the histone extracts was captured to the strip wells coated with anti-acetyl histone H4 antibody. The captured acetyl histone H4 can then be detected with a labeled detection antibody, followed by a color development reagent. When the color of the solution became blue, the stop solution was added to each well to stop the reaction. When the color changed from blue to yellow, the absorbance was recorded at 450 nm in a microplate reader (Epoch, BioTek Instruments, Winooski, VT, USA). Percent histone H4 acetylation was calculated as follows:

$$\%\ \text{Histone H4 acetylation} = \frac{\text{Treated sample OD} - \text{Blank OD}}{\text{Control OD} - \text{Blank OD}} \times 100$$

Isolation and culture of patient-derived primary breast cancer cells

After getting the formal approval of the Institutional Ethics Committee (Ethical clearance approval Regd. #ECR/297/Inst/OR/2013) of Acharya Harihar Regional Cancer Centre, Cuttack, Odisha, India, the patient-derived breast cancer tissues were collected from the cancer patients during surgery. Then the samples were further processed according to our laboratory protocol [24]. First, the tissue samples were washed with 1XPBS and cut into small pieces in a media containing three different antibiotics (7.54 µM ciprofloxacin, 0.26 µM amphotericin B, and 0.14 mM ampicillin). Then they were treated with 0.1% collagenase and 50U/mL dispase, followed by incubation for 2 h in 37 °C water bath with continuous rotating motion. Next, the fat bodies were removed from the cells by using a 40 µm cell strainer, and the cells were centrifuged at 1000 rpm for 10 min. The cells were seeded in 60 mm culture dishes with DMEM-F12 media, supplemented with 20% FBS, 1.5 mM L-glutamine and 2% antibiotic (100U/mL penicillin and 10 mg/mL streptomycin) and allowed to grow for 5 to 8 days under regular observation.

Hematoxylin and eosin (H and E) staining of patient-derived breast cancer tissues

H&E staining procedures were carried out as per protocol mentioned earlier [25]. In brief, 5 µm thick paraffin-embedded specimens were mounted on poly-L-lysine coated slides. The slides were heated at 60 °C for 30–40 min, followed by de-waxing with xylene and rehydrating with decreasing concentrations (100%, 90% and 70%) of ethanol. In H&E staining, the sections were first immersed in hematoxylin, then eosin and slowly washed with water. Then the sections were dehydrated with increasing concentrations of ethanol (70, 90, and 100%), and immersed for 2 min first in xylene and then in acetone. Next, the slides were processed by using the mounting medium (DPX) and coverslips. The images were recorded with the help of a brightfield microscope at 20X magnification (Leica DM200, USA).

Statistical analysis

Statistical data analysis was performed by using GraphPad Prism version 5 software, USA. The data were analyzed by one-way ANOVA wherever applicable and expressed as mean ± SD of at least three independent experiments. Statistical significance of differences was represented as '*' ($p < 0.05$), '**' ($p < 0.001$) and '***' ($p < 0.0001$), and 'ns' represents statistically non-significant mean differences.

Results

OLA effectively inhibits HR repair pathway mainly in the chromatin-bound fraction of RES-treated MCF-7 breast cancer cells

In our previous article, we showed that OLA enhances the apoptotic potentiality of RES by deregulating the HR repair pathway through catalytic inhibition and trapping of PARP1 in breast cancer cells. Inhibition of PARylation blocked PARP1-BRCA1 interaction, which resulted in inhibition of HR pathway [8]. Now question arises, whether RES + OLA combination treatment can effectively inhibit relaxation of the chromatin structure and thereby block the HR pathway proteins from accessing the DNA damage site. To address this issue, we first separated the chromatin fraction and the nuclear fraction in the MCF-7 cellular lysates to ascertain the exact subcellular location of RES + OLA-mediated inhibition of HR pathway. For that, we treated MCF-7 cells with RES, OLA and their combination and then observed for any changes in the expression of DNA repair pathway (HR, NHEJ, and BER) proteins in both nuclear and chromatin fractions of the cells (Fig. 1). In western blot analysis, it was found that after RES + OLA combination treatment, there was no significant change in the expression of the DNA repair proteins in the nuclear-bound fractions of MCF-7 cells, in comparison to the untreated control (Fig. 1**Ai**). On the other hand, in the chromatin fraction of the cells, upon RES treatment, there was an increase in the expressions of the HR pathway proteins, such as, MRE11 (2.1-fold), BRCA1 (2.5-fold), RPA70 (2.4-fold), BRCA2 (2.9-fold), and RAD51 (4.2-fold) as compared to the untreated control. But, after addition of OLA in RES-treated cells, a significant reduction in the expressions of MRE11 (10.5-fold), BRCA1 (25-fold), RPA70 (12-fold), BRCA2

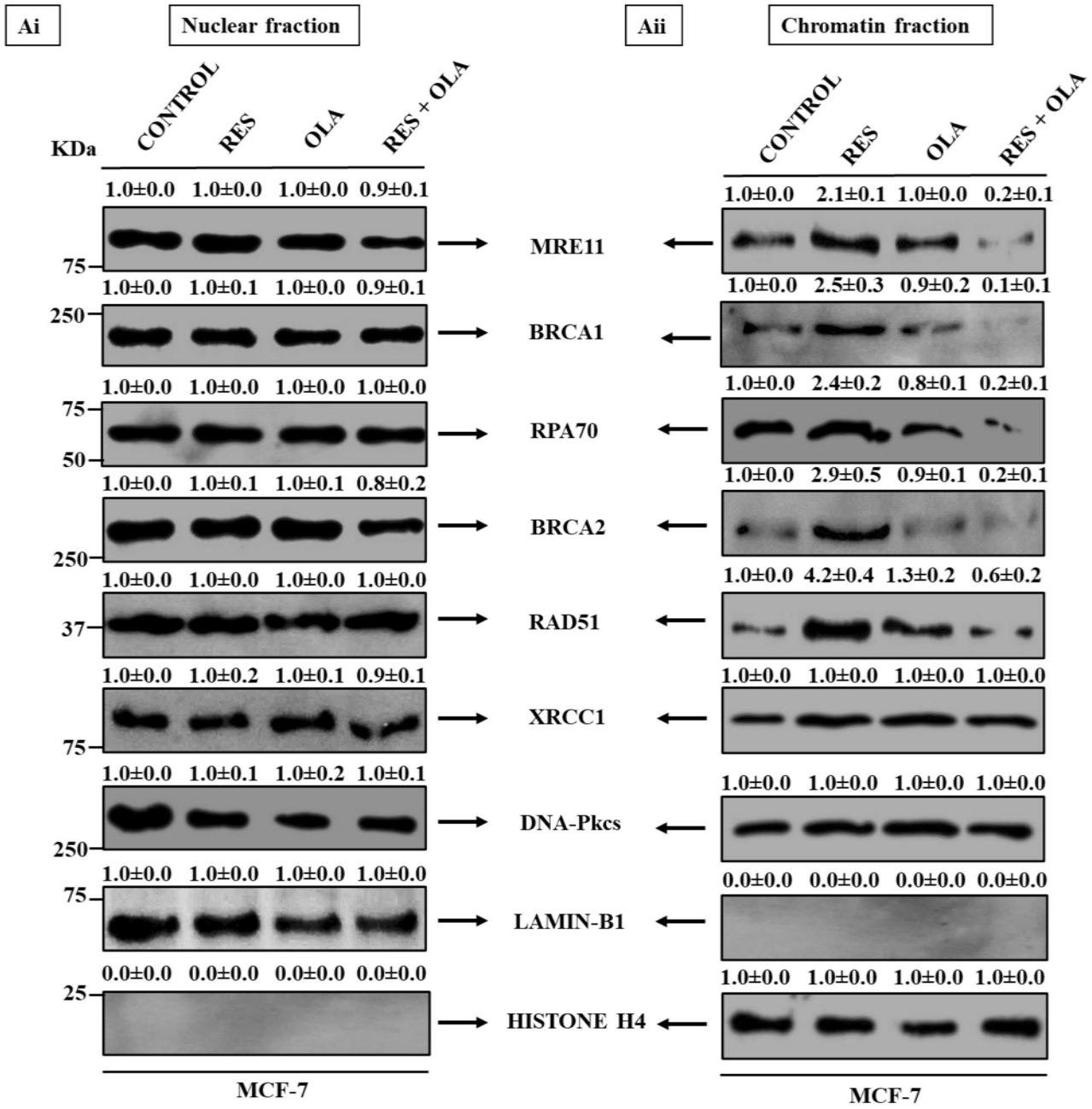

Fig. 1 OLA effectively inhibits HR repair pathway mainly in the chromatin-bound fraction of RES-treated MCF-7 breast cancer cells: MCF-7 cells were treated with individual and combination exposure of RES and OLA as mentioned in materials and methods section. After drug treatment, the nuclear and chromatin fractions of the cells were isolated and processed for western blot analysis. **Ai** Expressions of HR, BER and NHEJ cascade proteins in nuclear fraction of MCF-7 cells. **Aii** Expressions of HR, BER and NHEJ cascade proteins in chromatin fraction of MCF-7 cells. LAMIN-B1 and HISTONE H4 were used as loading control for nuclear and chromatin fractions, respectively. The numerical values above each blot represent the relative fold change with respect to control; the band intensity was measured by densitometric analysis. Blots were the best representative of the three independent experiments

(14.5-fold), and RAD51 (7-fold) was observed in comparison to the RES-treated cells. On the other hand, the expressions of XRCC1 and DNA-Pkcs, the major components of BER and NHEJ pathways, respectively were found to be unchanged in the combination drug-treated chromatin fraction of the cells (Fig. 1**Aii**). Thus, the above data suggested that RES + OLA-mediated HR repair pathway inhibition is majorly taking place in the chromatin-bound fraction and not in the rest of the nucleus.

In DNA damage response, PARP-1 plays an important role in directly recognizing the DNA damage and catalyzing the synthesis of PAR polymers, which form a scaffold

and help in the recruitment of the DNA repair proteins at the DNA damage site. Hence, it was imperative to check the effect of OLA on PARP-1 mediated PARylation and HR pathway proteins in the nuclear and chromatin fractions of RES pre-treated MCF-7 cells. Basal level signal of PAR chain formation and expressions of HR pathway proteins

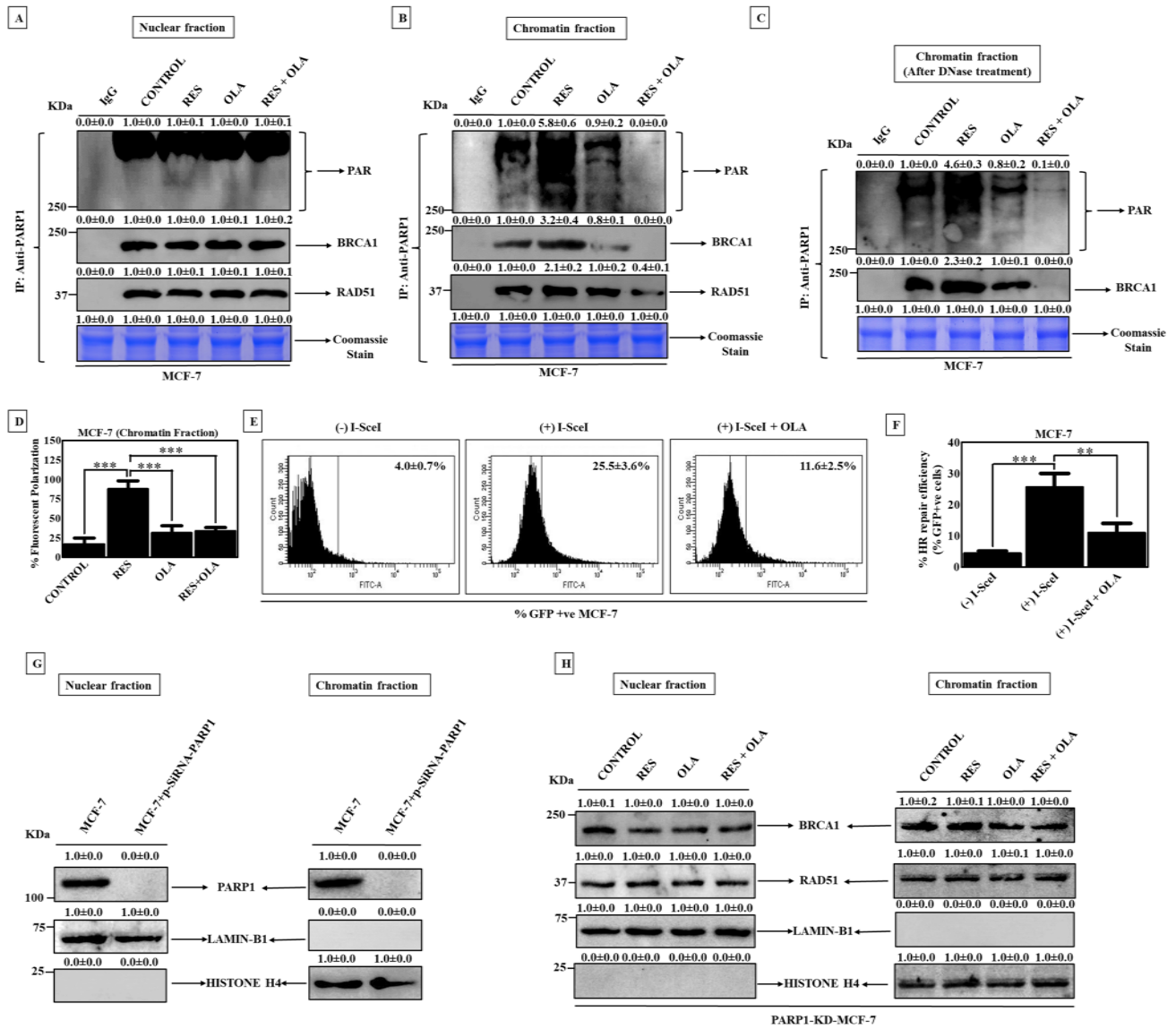

Fig. 2 RES + OLA combination treatment inhibited PARP1-mediated PARylation, trapped PARP1 at DNA damage site and terminated PARP1-BRCA1 interaction in chromatin fraction of MCF-7 cells. RES + OLA also blocked the HR pathway in MCF-7 cells: **A** and **B** Expressions of PAR, BRCA1, and RAD51 in RES, OLA, and RES + OLA treated PARP-1 immunoprecipitated nuclear and chromatin fractions of MCF-7 cells, respectively. **C** PARP1-immunoprecipitated chromatin fractions of MCF-7 cells were treated with DNase and then the expressions of PAR and BRCA1 were checked. IgG was used as a negative control and the coomassie stained gel represents the equal loading of protein in the blots. The numerical value above each panel of the blots showed the relative fold change with respect to control. The band intensity was measured by densitometric analysis. The blots have been represented as the results of three independent experiments. **D** MCF-7 cells were treated with RES, OLA, and RES + OLA, and the chromatin fractions were isolated, followed by the analysis of their fluorescent polarization (FP). The bar graph shows the percentage of FP of chromatin fractions of drug-treated cells. **E** Percentage of GFP + ve cells to measure the HR pathway efficiency in (−) I-SceI, (+) I-SceI, and (+) I-SceI + OLA treated MCF-7 cells. **F** Bar graph representing the percentage of GFP + ve cells observed in E. **(G)** PARP1 protein expression in nuclear and chromatin fractions of MCF-7 + siRNA-scrambled and MCF-7 + siRNA-*parp1* cells. **H** Expressions of selected HR proteins (BRCA1 and RAD51) in nuclear and chromatin fractions of PARP1-KD-MCF-7 cells after exposure to RES, OLA and RES + OLA. LAMIN-B1 and HISTONE H4 were used as loading control for nuclear and chromatin fractions, respectively. The data were calculated as the mean ± SD of three separate experiments (n = 3). The statistical analysis was performed using Graph Pad Prism version 5 software, USA. Statistical significance of difference in the central tendencies compared to the controls was designated as *$p < 0.05$, **$p < 0.001$ and ***$p < 0.0001$

(BRCA1 and RAD51) were noted in the nuclear fraction of PARP1-immunoprecipitated MCF-7 cells before and after drug treatments (Fig. 2A). On the other hand, it was noted that there was a 5.8-fold increase in PARylation in the chromatin fraction of PARP1-immunoprecipitated cells after 30 h exposure of RES compared to untreated control. Interestingly, complete abolishment of PARylation was seen after 24 h exposure of OLA in RES 6 h pretreated cells as compared to 30 h RES-treated MCF-7 cells. Inhibition of PARylation stopped the interaction between PARP1 and BRCA1, which caused complete downregulation of BRCA1. Inhibition of PARP1-BRCA1 interaction resulted in a 5.2-fold decrease in the expression of another HR protein RAD51 in the chromatin fraction of RES + OLA-treated PARP1-immunoprecipitated cells in comparison to RES-treated MCF-7 cells (Fig. 2B). The PARP1-BRCA1 interaction could be mediated by DNA and hence the PARP1-immunoprecipitated samples were treated with DNase to validate this interaction. 10-fold reduced signal of PAR chain formation and complete downregulation of BRCA1 were observed after RES + OLA treatment in DNase-treated IP samples in comparison to untreated control (Fig. 2C).

The above experiments indicated that OLA treatment efficiently inhibited the catalytic activity of PARP-1 in the chromatin fraction of RES pre-treated MCF-7 cells. Hence, it was important to also assess whether RES + OLA combination treatment could trap PARP-1 at the DNA damage site in the chromatin fraction of the cells. In the fluorescence anisotropy PARP trapping assay, the PARP trapping potentiality is found to be indirectly proportional to the amount of free PARPs available in the system, which can be measured by estimating the fluorescence polarization (FP) produced after binding to an externally-added fluorescent-labeled nicked DNA. Following addition of the nicked DNA, external PARP inhibitor (OLA) and NAD^+ in RES-treated chromatin lysates, there was an approximately 6-fold ($p < 0.0001$) increase in %FP as compared to untreated control. This increase in %FP can be attributed to high free PARP availability, and less cellular PARP trapping after RES treatment. But, in RES + OLA treated chromatin lysates, there was a 2.4-fold ($p < 0.0001$) decrease in %FP in comparison to RES-treated chromatin lysates (Fig. 2D). This suggested that there was less free PARP availability, and more cellular PARP trapping after addition of OLA in RES pre-treated cells, resulting in accumulation of DSBs in the cells due to HR pathway inhibition.

Next, to directly measure the HR pathway activity in the cells before and after DSB induction, the DR-GFP reporter plasmid-based HR efficiency assay was performed. It was found that there was a significant decrease in the HR pathway activity after OLA treatment in pCBASceI endonuclease-transfected MCF-7 cells. First, the DR-GFP plasmid-transfected MCF-7 cells showed 4% GFP-positive cell population. But after pCBASceI endonuclease transfection, the percentage of GFP-positive cell population increased to 25.5%, which indicated increase in HR pathway activity in the cells. Then, OLA treatment in pCBASceI-transfected cells caused reduction in GFP-positive cells to 11.6%. This decrease in GFP-positive cell population clearly suggested that addition of OLA in the endonuclease-transfected cells efficiently inhibited the HR pathway activity (Fig. 2E). In Fig. 2F, the bar graph showed that there was a 6.3-fold ($p < 0.0001$) increase in %GFP + ve cells after pCBASceI endonuclease transfection as compared to only pDR-GFP-transfected cells. But after OLA treatment in endonuclease-transfected cells, there was a 2.2-fold ($p < 0.001$) decrease in %GFP + ve cells in comparison to the endonuclease-transfected cells. This implied that OLA caused PARP inhibition, and in turn interfered with the HR pathway activity, which stopped the cells from repairing the endonuclease-induced DSB.

To know the role of PARP1 more precisely, the PARP1 gene was first knocked down in MCF-7 cells using p-SiRNA-*parp1* plasmid. Western blot analysis revealed abolishment of PARP1 in both nuclear and chromatin fractions of p-SiRNA-*parp1* plasmid transfected MCF-7 cells (PARP1-KD-MCF-7) (Fig. 2G). Further, the expression levels of selected HR proteins (BRCA1 and RAD51) were checked in PARP1-silenced MCF-7 cells, where unchanged BRCA1 and RAD51 expressions were found in nuclear and chromatin fractions of PARP1-silenced cells both before and after drug treatments (Fig. 2H). Hence, the above experimental findings revealed that the DNA repair pathway inhibition and OLA-mediated PARP1 trapping are PARP1-dependent processes.

BRCA1 knockdown completely abolishes the HR pathway in the chromatin fraction of RES + OLA-treated MCF-7 breast cancer cells

The previous experiments clearly suggested that OLA treatment inhibited the formation of PAR chains at the DNA damage site in the chromatin fractions of RES pre-treated cells, resulting in termination of PARP1-BRCA1 interaction and downregulation of HR pathway proteins. To understand the role of BRCA1 in PARP1-mediated HR pathway activation, the BRCA1 gene was silenced by using p-SiRNA-*brca1* plasmid. Western blot analysis showed complete knockdown of BRCA1 in both nuclear and chromatin fractions of p-SiRNA-*brca1* plasmid transfected MCF-7 cells (BRCA1-KD-MCF-7) (Fig. 3A). Next, the expression levels of selected HR pathway proteins (MRE11, RPA70, BRCA2, and RAD51) were checked in both nuclear and chromatin fractions of BRCA1-KD-MCF-7 cells, where their expressions were found to remain unchanged both before and after drug treatments

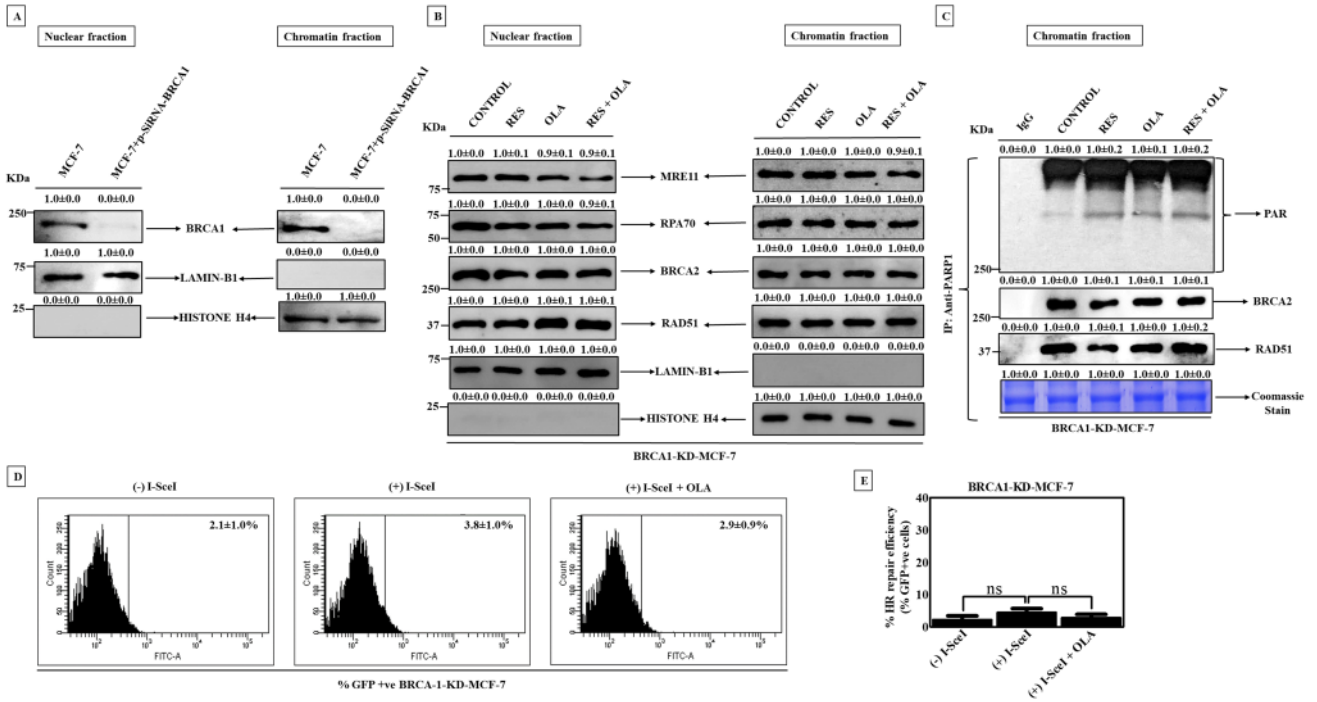

Fig. 3 BRCA1 knockdown completely abolishes the HR pathway in the chromatin fraction of RES + OLA-treated MCF-7 breast cancer cells: A BRCA1 protein expression in nuclear and chromatin fractions of MCF-7 + siRNA-scrambled and MCF-7 + siRNA-*brca1* cells. **B** Expressions of selected HR proteins in nuclear and chromatin fractions of BRCA1-KD-MCF-7 cells after exposure to RES, OLA and RES + OLA. LAMIN-B1 and HISTONE H4 were used as loading control for nuclear and chromatin fractions, respectively. **C** Expressions of PAR and selected HR proteins in the chromatin fraction of PARP1-immunoprecipitated BRCA1-KD-MCF-7 cells before and after RES, OLA, and RES + OLA treatments. IgG was used as a negative control and the coomassie stained gel represents the equal loading of protein in the blots. The numerical value above each panel showed the relative fold change with respect to control. The band intensity was measured by densitometric analysis. **D** Percentage of GFP + ve cells to measure the HR pathway efficiency in (−) I-SceI, (+) I-SceI, and (+) I-SceI + OLA treated BRCA1-KD-MCF-7 cells. **E** Bar graph representing the percentage of GFP + ve cells observed in D. The blots have been represented as the results of three independent experiments. The data were calculated as the mean ± SD of three separate experiments (n = 3). The statistical analysis was performed using Graph Pad Prism version 5 software, USA. Statistical significance of difference in the central tendencies compared to the controls was designated as $^{*}p < 0.05$, $^{**}p < 0.001$ and $^{***}p < 0.0001$, and 'ns' represents statistically non-significant mean differences

(Fig. 3B). Then, PARP1 was immunoprecipitated in the chromatin fractions of RES, OLA, and RES + OLA treated BRCA1-silenced cells to investigate any changes in PARP1-mediated PARylation. Basal level signal of PAR chain formation was observed after immunoprecipitation of PARP1 in the chromatin fraction of BRCA1-KD-MCF-7 cells. Immunoprecipitation study was also performed to check the physical interaction of PARP1 with HR proteins (BRCA2 and RAD51) in chromatin fraction of BRCA1-silenced cells. Unchanged interactions of PARP1 with BRCA2 and RAD51 were noted in BRCA1-KD-MCF-7 cells (Fig. 3C). Next, it was imperative to assess the HR pathway activity in the BRCA1-KD-MCF-7 cells. In the HR efficiency assay, due to BRCA1 silencing and complete abolishment of HR pathway, there was not much increase in %GFP + ve cell population (4.5%) after DSB induction by pCBASceI transfection in pDR-GFP-transfected cells, in comparison to 2.1% GFP + ve cells after only pDR-GFP transfection. Then, OLA treatment in pCBASceI-transfected BRCA1- KD-MCF-7 cells reduced the %GFP + ve cell population to 2.9% (Fig. 3D). The bar graph in Fig. 3E showed that there was an approximately 1.8-fold ($p > 0.05$) increase in %GFP + ve cells after pCBASceI endonuclease transfection as compared to only pDR-GFP-transfected cells. But after OLA treatment in endonuclease-transfected cells, there was a 1.5-fold ($p > 0.05$) decrease in %GFP + ve cells in comparison to the endonuclease-transfected cells. The above experimental data clearly suggested that BRCA1 plays a very important role in PARP1-mediated HR pathway activation in the chromatin fraction of MCF-7 cells and OLA treatment effectively inhibits the HR pathway in RES pre-treated cells by terminating the interaction between PARP1 and BRCA1.

RES + OLA combination treatment blocks HR repair pathway in MCF-7 cells through inhibition of TIP60-mediated relaxation of chromatin assembly

The chromatin assembly, which holds together the DNA and other histone and non-histone proteins, is a compact network which acts as a physical barrier to protect the DNA from different proteins involved in replication, transcription, and DNA repair processes. When a cell suffers DNA damage, the chromatin network is relaxed so that the DNA repair proteins can get access to the site containing the DNA lesion. It was previously shown in Fig. 1Aii and Fig. 2B that RES + OLA combination treatment caused a significant reduction in PARylation, and downregulation of HR pathway proteins in the chromatin fraction of MCF-7 cells. This led us to hypothesize that there might be an interlink between chromatin remodeling and activation of HR repair pathway, which then directs the repair of DSBs in the chromatin. During chromatin remodeling, the histone acetyltransferases (HAT) induce the acetylation of histone proteins, which result in relaxation of the chromatin network. One of the most important HAT enzymes involved in DSB repair is TIP60, which is known to hyperacetylate H4 histone proteins. Hence, it was imperative to check whether there was any change in the activity of the HAT enzymes before and after drug treatments. First, the HAT activity assay was performed to measure the activity of histone acetyltransferases, such as TIP60, in the nuclear extracts of MCF-7 cells treated with individual and combination treatments of RES and OLA. It was observed that individual RES treatment caused approximately 2-fold ($P < 0.0001$) increase in the HAT activity as compared to untreated control. On the other hand, RES + OLA treatment caused 7-fold ($P < 0.0001$) reduction in HAT activity in comparison to the RES-treated cells (Fig. 4A). Next, it was crucial to assess any changes in the HAT-mediated acetylation of H4 histone proteins in MCF-7 cells. In the H4 total acetylation colorimetric assay, there was an approximately 2-fold ($p < 0.001$) increase in H4 acetylation post RES treatment as compared to untreated control. But, after RES + OLA treatment, H4 acetylation levels were decreased by 4.4-fold ($p < 0.0001$) in comparison to the RES-treated cells (Fig. 4B). In western blot analysis, the expressions of the HAT enzyme TIP60, motor ATPase P400 protein, and H4 acetylated products H4K5ac and H4K8ac were all significantly increased by 4.1-, 3.2-, 2.4-, and 3.1-fold, respectively in the chromatin fraction of RES-treated MCF-7 cells as compared to untreated control. But, after RES + OLA treatment, there was complete downregulation in the expressions of TIP60, P400, H4K5ac, and H4K8ac in comparison to the RES-treated cells (Fig. 4C). Next, the immunoprecipitation assay was performed to investigate whether there was any interaction of TIP60 with PARylated PARP1 and selected HR proteins (BRCA1 and RAD51) in the chromatin fraction of RES, OLA, and RES + OLA treated MCF-7 cells. Following the immunoprecipitation of TIP60, there was a significant increase in the signal of PAR chain formation (4.4-fold), and the expressions of BRCA1 (3.8-fold), and RAD51 (2.1-fold) after individual RES treatment in comparison to untreated control. But, after RES + OLA treatment, the signal of PAR chain formation and BRCA1 expression were completely downregulated in the chromatin fraction of the TIP60-immunoprecipitated cells. This implied that PARP1-mediated interaction between TIP60 and BRCA1 was terminated after RES + OLA treatment in MCF-7 cells. Inhibition of PARP1-BRCA1 interaction resulted in a 3.5-fold decrease in the expression of RAD51 in the chromatin fraction of RES + OLA-treated TIP60-immunoprecipitated cells in comparison to RES-treated cells (Fig. 4D). Further, to confirm the co-localization of BRCA1 and TIP60 in MCF-7 cells, an immunofluorescence assay was performed. The microscopic images showed that after RES treatment, BRCA1 and TIP60 expressions were significantly upregulated as compared to control and they were co-localizing with each other in the cells. But, after RES + OLA combinatorial exposure, their expressions were markedly downregulated, in comparison to only RES-treated cells (Fig. 4E). When the fluorescence signals obtained for BRCA1 and TIP60 were quantified and plotted on a graph, the number of merged cells was found to be increased by approximately 5-fold ($p < 0.0001$) after RES individual treatment in comparison to untreated control. But after RES + OLA treatment, the number of merged cells was reduced 11-fold ($p < 0.0001$) approximately, as compared to RES treatment (Fig. 4F). Next, to check whether RES + OLA was affecting the chromatin relaxation process, the expression of acetylated histone H4K5ac was assessed by performing an immunofluorescence assay. It was observed that the expression of H4K5ac was significantly upregulated after RES exposure in comparison to untreated control. This clearly suggested that RES treatment caused significant amount of DNA damage, which induced activation of the chromatin relaxation process as evident from the remarkable increase in the expression of histone H4 acetylated product. But after RES + OLA treatment, H4K5ac expression was markedly reduced in comparison to that observed in RES-treated cells (Fig. 4G). Relative H4K5ac expression was shown in Fig. 4H and the data showed that there was an approximately 5.5-fold ($p < 0.0001$) increase in the expression of H4K5ac after RES individual treatment, in comparison to untreated control. But, after RES + OLA combination treatment, H4K5ac expression was downregulated by approximately 13-fold ($p < 0.0001$), in comparison to RES individual treatment. This implied that addition of OLA in RES-treated cells terminated the interaction between PARylated PARP1 and TIP60, which blocked the histone acetylation process, resulting in the reduction of acetylated histone

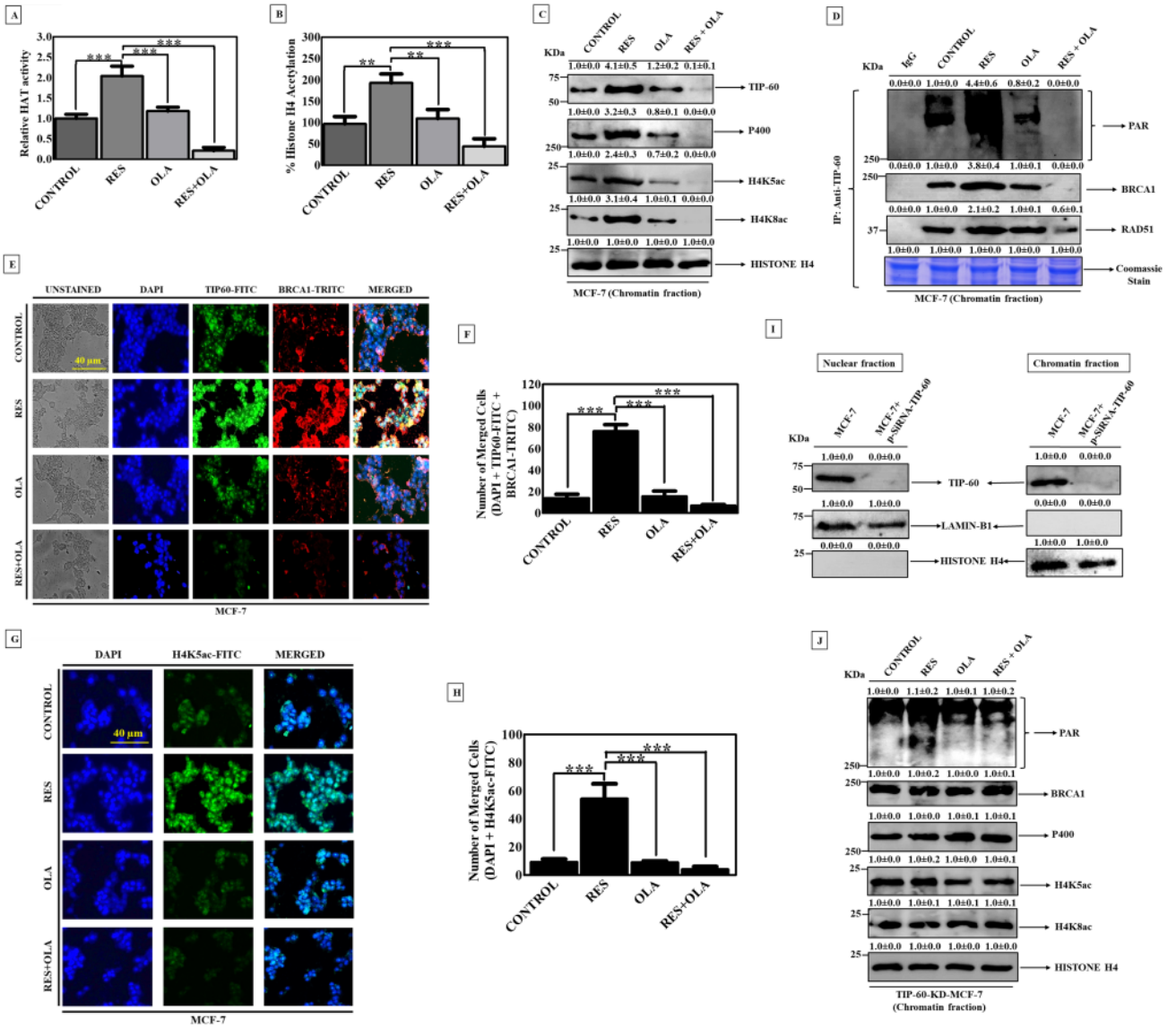

H4 expression. Further, to understand the role of TIP60 in PARP1-mediated HR pathway activation, the TIP60 gene was silenced by using p-SiRNA-*tip60* plasmid. Western blot analysis showed complete knockdown of TIP60 in both nuclear and chromatin fractions of p-SiRNA-*tip60* plasmid transfected MCF-7 cells (TIP60-KD-MCF-7) (Fig. 4I). Next, the signal of PAR chain formation, and the expressions of BRCA1, P400, and H4K5ac and H4K8ac were checked in the chromatin fraction of TIP60-KD-MCF-7 cells, where their expressions were found to remain unchanged both before and after drug treatments (Fig. 4J). Altogether, the above data suggested that RES + OLA combination efficiently trapped PARP1 at the DSB-containing site and simultaneously inhibited the function of TIP60 histone acetylation enzyme, stopped H4 acetylation, and completely deregulated the chromatin relaxation process. This, in turn, affected the cooperative interaction between PARP1, TIP60 and BRCA1, which resulted in complete inhibition of the HR pathway in MCF-7 cells.

RES + OLA combination treatment inhibits TIP60-mediated chromatin relaxation and blocks HR repair pathway in patient-derived primary breast cancer cells

From the experimental results obtained under in vitro conditions, it was evident that the RES + OLA combination treatment can catalytically inhibit and trap PARP1 at the DNA damage site, and block the TIP60-mediated relaxation of the chromatin assembly to completely stop the HR pathway activity in MCF-7 cells. To further confirm the above results, some of the experiments were performed again

◂**Fig. 4** RES + OLA combination treatment terminates cooperative interaction between PARP1, TIP60, and BRCA1 and inhibits TIP60-mediated chromatin relaxation in MCF-7 breast cancer cells: A Bar graph representing the relative HAT enzymatic activity in the nuclear extracts of MCF-7 cells before and after RES, OLA, and RES + OLA treatments. **B** Bar graph showing the percentage of histone H4 acetylation in the histone extracts of MCF-7 cells before and after RES, OLA, and RES + OLA treatments. **C** Expressions of TIP60, P400, and the acetylated products of histone H4 (H4K5ac and H4K8ac) in the chromatin fraction of RES, OLA, and RES + OLA treated MCF-7 cells. HISTONE H4 was used as loading control for chromatin fraction. **D** Expressions of PAR and selected HR proteins in the chromatin fraction of TIP60-immunoprecipitated MCF-7 cells before and after RES, OLA, and RES + OLA treatments. IgG was used as a negative control and the coomassie stained gel represents the equal loading of protein in the blots. The numerical value above each panel showed the relative fold change with respect to control. The band intensity was measured by densitometric analysis. **E** Co-localization of BRCA1 and TIP60 in MCF-7 cells measured by fluorescence microscopy. Extreme left panel showed unstained, middle three panels represent DAPI, BRCA1-FITC and TIP60-TRITC, and the extreme right panel showed the merged images representing co-localization of BRCA1 and TIP60. **F** Bar graph representing the quantitation of fluorescence signals obtained in merged cells (DAPI + TIP60-TRITC + BRCA1-FITC) of E. **G** Immunocytochemical staining of H4K5ac in RES, OLA, and RES + OLA treated MCF-7 cells. Images were taken using fluorescence microscope at 40X magnification (scale bar 40 µm). Data was the representative of three independent experiments. **H** Bar graph representing the quantitation of H4K5ac expression in merged cells (DAPI + H4K5ac-TRITC) of G. **I** TIP60 protein expression in nuclear and chromatin fractions of MCF-7 + siRNA-scrambled and MCF-7 + siRNA-*tip60* cells. **J** Expressions of PAR, BRCA1, P400, and the acetylated products of histone H4 (H4K5ac and H4K8ac) in the chromatin fractions of TIP60-KD-MCF-7 cells after exposure to RES, OLA, and RES + OLA. HISTONE H4 was used as a loading control for the chromatin fraction. The blots have been represented as the results of three independent experiments. The data were calculated as the mean ± SD of three separate experiments (n = 3). The statistical analysis was performed using Graph Pad Prism version 5 software, USA. Statistical significance of difference in the central tendencies compared to the controls was designated as *$p < 0.05$, **$p < 0.001$ and ***$p < 0.0001$

in patient-derived primary breast cancer cells. Tumor tissues and the adjacent normal tissues were collected from breast cancer patients, and used in the following experiments. Hematoxylin and eosin (H and E) staining showed a significant increase in the nucleus-to-cytoplasm ratio and the number of polymorphic nuclei in the tumor tissue as compared to uniform tissue architecture of healthy adjacent tissue (Fig. 5A). Next, the cancer cells were isolated from the breast cancer tissues, cultured, and then treated with RES, OLA, and RES + OLA combination (Fig. 5B). Then the nuclear and chromatin fractions were separated from the cellular lysates and the expressions of TIP60, P400, H4K5ac, and H4K8ac were checked in the chromatin fractions of primary breast cancer cells. It was found that all the above-mentioned proteins were completely downregulated after RES + OLA combination treatment in comparison to untreated control (Fig. 5C). Next, the immunoprecipitation assay was performed in the chromatin fraction of TIP60-immunoprecipitated cells to look for any interaction between TIP60 and PARylated PARP1 and the HR pathway protein BRCA1. It was found that after individual RES exposure, the signal of PAR chain formation and the expression of BRCA1 were significantly increased by 6.1- and 3.4-fold, respectively as compared to untreated control. But, exposure of OLA in RES pre-treated cells caused a complete downregulation of both PAR and BRCA1 in comparison to RES-treated cells. This clearly suggested that TIP60 physically interacts with PARylated PARP1 and BRCA1, which was terminated after RES + OLA treatment (Fig. 5D). In the fluorescence anisotropy PARP trapping assay, when the fluorescence-tagged nicked DNA, external PARP inhibitor (OLA) and NAD^+ were added in the chromatin fraction of RES-treated primary breast cancer cells, there was an approximately 8-fold ($p < 0.0001$) increase in %FP as compared to untreated control. But, in RES + OLA treated chromatin lysates, there was a 2.7-fold ($p < 0.001$) decrease in %FP in comparison to RES-treated chromatin lysates. This suggested that with the reduction in %FP, there was less free PARP availability, and more cellular PARP trapping after addition of OLA in RES pre-treated cells (Fig. 5E). In plasmid-based HR efficiency assay, after pDR-GFP transfection in primary breast cancer cells, percentage of GFP-positive cells was found to be 5.8%. Post pCBASceI endonuclease transfection, the %GFP-positive cell population increased to 29.1%, which implied that I-SceI-induced DSB enhanced the HR pathway activity in the primary breast cancer cells. Then, OLA treatment in pCBASceI-transfected cells decreased the %GFP-positive cell population to 13.5%, which suggested that addition of OLA caused PARP inhibition, and in turn deregulated the HR pathway activity (Fig. 5F). The bar graph in Fig. 5G showed that there was an approximately 5-fold ($p < 0.0001$) increase in %GFP + ve cells after pCBASceI endonuclease transfection as compared to only pDR-GFP-transfected primary breast cancer cells. But after OLA treatment in ISceI-transfected cells, there was an approximately 2-fold ($p < 0.001$) decrease in %GFP + ve cells in comparison to the endonuclease-transfected cells.

Discussion

Inside a eukaryotic cell, the DNA molecule is found to be tightly packaged along with histone and non-histone proteins in a compact chromosomal material called chromatin. This chromatin assembly forms a protective layer around the DNA to avoid unwanted interactions with different cellular proteins. But, when a cell suffers a DNA damage, this compact chromatin network is known to relax and open, so that the proteins involved in different DNA repair pathways can get an access and bind to the DNA damage site. This

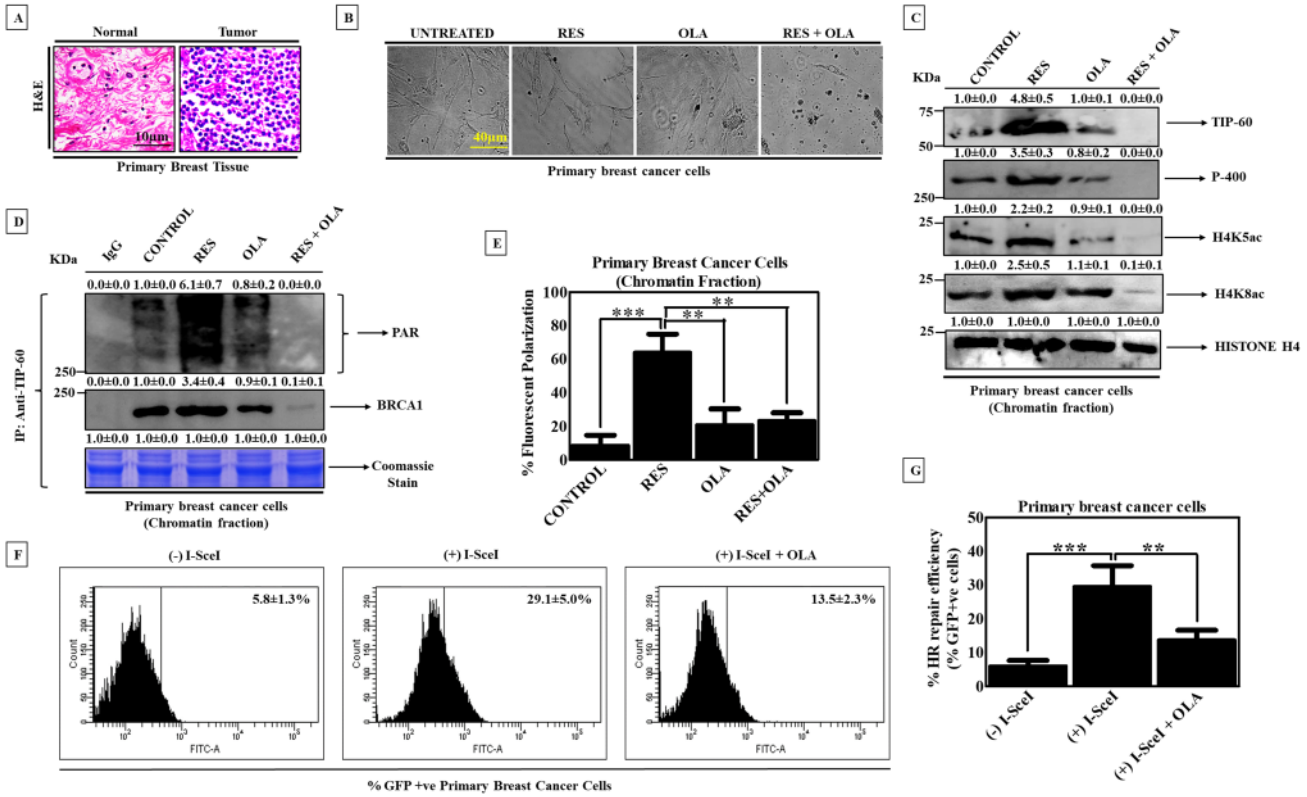

Fig. 5 RES + OLA combination treatment inhibits TIP60-mediated chromatin relaxation and blocks HR pathway in patient-derived primary breast cancer cells: **A** H and E staining of normal and malignant forms of primary breast tissue. **B** Morphology of human primary breast cancer cells before and after RES, OLA, and RES + OLA combination treatments. **C** Expression of TIP60, P400, and the acetylated products of histone H4 (H4K5ac and H4K8ac) in the chromatin fraction of primary breast cancer cells after treatment with RES, OLA, and RES + OLA. HISTONE H4 was used as a loading control for the chromatin fraction. **D** Expressions of PAR and BRCA1 in the chromatin fraction of TIP60-immunoprecipitated primary breast cancer cells before and after RES, OLA, and RES + OLA treatments. IgG was used as a negative control and the coomassie stained gel represents the equal loading of protein in the blots. The numerical value above each panel showed the relative fold change with respect to control. The band intensity was measured by densitometric analysis. **E** Primary breast cancer cells were treated with RES, OLA, and RES + OLA, and the chromatin fractions were isolated, followed by the analysis of their fluorescent polarization (FP). The bar graph shows the percentage of FP of chromatin fractions of drug-treated cells. **F** Percentage of GFP + ve cells to measure the HR pathway efficiency in (−) I-SceI, (+) I-SceI, and (+) I-SceI + OLA treated primary breast cancer cells. **G** Bar graph representing the percentage of GFP + ve cells observed in F. The blots have been represented as the results of three independent experiments. The data were calculated as the mean ± SD of three separate experiments (n = 3). The statistical analysis was performed using Graph Pad Prism version 5 software, USA. Statistical significance of difference in the central tendencies compared to the controls was designated as *$p < 0.05$, **$p < 0.001$ and ***$p < 0.0001$

process is called chromatin remodeling and it requires the action of different multi-subunit remodeling complexes to maintain the dynamic nature of the chromatin assembly [3]. One such remodeling complex is the human NuA4 (hNuA4) complex, which is found to be highly active after induction of DSBs in a cell. It has multiple subunits, including the HAT enzyme TIP60, P400 motor ATPase, and Ruvbl1 and Ruvbl2 helicase-like proteins. P400 facilitates destabilization of the nucleosomes around the DSB site, which helps TIP60 to catalyze the acetylation of H4 histones. H4 hyperacetylation results in chromatin relaxation that gives access to the HR pathway proteins to bind to the DSB site [14, 16]. Now, in our recently published article, we have shown that 10 μM RES treatment for 6 h caused generation of DSBs in breast cancer cells, followed by 4nM OLA exposure for 24 h, which efficiently enhanced RES-induced DSBs, inhibited the HR pathway proteins, caused a late S/G2 cell cycle arrest, and apoptosis in RES pre-treated breast cancer cells [8]. But we did not check whether this HR pathway inhibition was taking place within the chromatin assembly or in the rest of the nucleus. Hence, it was important to investigate whether RES + OLA combination treatment blocked the HR pathway proteins from accessing and binding to the DSB site through inhibition of chromatin relaxation or by changing the orchestra in the nucleus.

Here, in the present study, we have performed multiple experiments in in vitro (MCF-7) and ex vivo (patient-derived primary breast cancer cells) preclinical model systems to

delineate the mechanism of RES + OLA-mediated inhibition of relaxation of chromatin assembly to block the HR pathway and cause breast cancer cell death. Apart from the in vitro experiments, the reason for using the ex vivo patient-derived primary breast cancer cells is the presence of a tumor microenvironment, which is known to contain cancer cells, tumor stromal cells, infiltrating inflammatory cells and several associated tissue cells that help in development of drug resistance, tumor escape and progression.

First, we checked whether RES + OLA combination treatment inhibited the HR pathway proteins in the nuclear or the chromatin fraction of MCF-7 breast cancer cells. It was found that RES + OLA effectively downregulated the expressions of representative HR proteins like MRE11, BRCA1, RPA70, BRCA2, and RAD51 only in the chromatin fraction, and not in the nuclear fraction. The expressions of some representative proteins of other repair pathways (XRCC1 in BER, and DNA-Pkcs in NHEJ) remained unchanged in both nuclear and chromatin fractions. This gave us an indication that the HR repair pathway was predominantly operating in the chromatin (Fig. 1).

To further confirm this experimental finding, the immunoprecipitation assays were performed in both nuclear and chromatin fractions of MCF-7 cells, which showed that inhibition of PARylation and abolition of PARP1-BRCA1 interaction took place only in RES + OLA-treated chromatin fraction of PARP1-immunoprecipitated cells. Apart from effective inhibition of the catalytic activity of PARP1, RES + OLA combination also efficiently trapped PARP1 at the DNA damage site in the chromatin fraction of the cells. In the DR-GFP reporter plasmid-based HR efficiency assay, it was found that OLA treatment in pCBASceI-transfected cells resulted in downregulation of HR activity. Next, it was important to confirm the role of PARP1 in RES + OLA-mediated HR inhibition. After PARP1 gene was knocked down in MCF-7 cells, both nuclear and chromatin fractions showed unaltered expressions of the HR pathway proteins. The above data suggested that RES + OLA-mediated HR pathway inhibition and PARP1 trapping were PARP1-dependent processes and these phenomena were predominantly taking place within the chromatin assembly (Fig. 2).

Since RES + OLA combination treatment was found to abolish PARP1-BRCA1 interaction in the chromatin fraction of MCF-7 cells, it was crucial to understand the role of BRCA1 in PARP1-mediated HR pathway activation. BRCA1 knockdown showed unaltered expressions of the HR pathway proteins in both nuclear and chromatin fractions of MCF-7 cells. Immunoprecipitation assay in PARP1-immunoprecipitated chromatin fraction of BRCA1-KD-MCF-7 cells showed no change in PAR signal and the expressions of HR proteins such as BRCA2 and RAD51. In the GFP plasmid-based HR efficiency assay, %GFP-positive cell population did not show any significant increase after DSB induction. Taken together, the experimental data clearly indicated that BRCA1 plays a very important role in PARP1-mediated HR pathway activation, knockdown of which resulted in complete inhibition of HR pathway in the chromatin fraction of MCF-7 cells (Fig. 3).

Previous results have shown that RES + OLA combination treatment terminated the interaction between PARP1 and BRCA1 in the chromatin fraction of the cells, resulting in inhibition of the HR pathway. Here, the major question arises that whether the process of chromatin remodeling is playing any role in this RES + OLA-mediated HR inhibition. It has been reported that HR is facilitated by histone acetyltransferases, such as TIP60, which promotes acetylation of H4 histones and thereby activates relaxation of the chromatin assembly. This allows the HR proteins to access the DSB site and repair the DNA lesion. Hence, inhibiting this process of chromatin relaxation is an effective approach to stop the cell's internal machinery from repairing the DNA damage. First, in the HAT activity assay and H4 total acetylation colorimetric assay, it was observed that RES + OLA treatment caused significant reduction in HAT activity and HAT-mediated H4 acetylation. In western blot analysis, the expressions of the HAT enzyme TIP60, motor ATPase P400 protein, and H4 acetylated products H4K5ac and H4K8ac were all downregulated in the chromatin fraction of RES + OLA-treated MCF-7 cells. This implied that recruitment of chromatin remodelers is entirely dependent on PARP1-mediated PARylation, and RES + OLA may block HR pathway by inhibiting chromatin relaxation. Moreover, this combinatorial exposure also terminated the physical interaction between TIP60, PAR, and BRCA1, suggesting that the association of TIP60 and the HR pathway protein BRCA1 is dependent on PARP1-mediated PARylation. Further, by performing immunofluorescence assays, RES + OLA combination treatment was found to significantly decrease the expressions of BRCA1, TIP60, and H4K5ac, in comparison to only RES-treated cells. Then, to understand the role of TIP60 in PARP1-mediated HR pathway activation, in TIP60-silenced condition, unchanged expressions of PAR, BRCA1, P400, H4K5ac and H4K8ac were observed in the chromatin fraction of TIP60-KD-MCF-7 cells both before and after drug treatments. Hence, the above data clearly suggested that RES + OLA combination treatment inhibited PARP1-mediated PARylation and trapped PARP1 at the DSB site, which resulted in blockade of TIP60-mediated chromatin relaxation and complete inhibition of the HR pathway in MCF-7 cells (Fig. 4).

Next, it was imperative to check whether the combinatorial exposure of RES and OLA can inhibit the process of chromatin relaxation and thereby block the HR pathway in the ex vivo patient-derived primary breast cancer cells. RES + OLA was found to significantly reduce the expressions of the HAT enzyme TIP60, P400 motor ATPase,

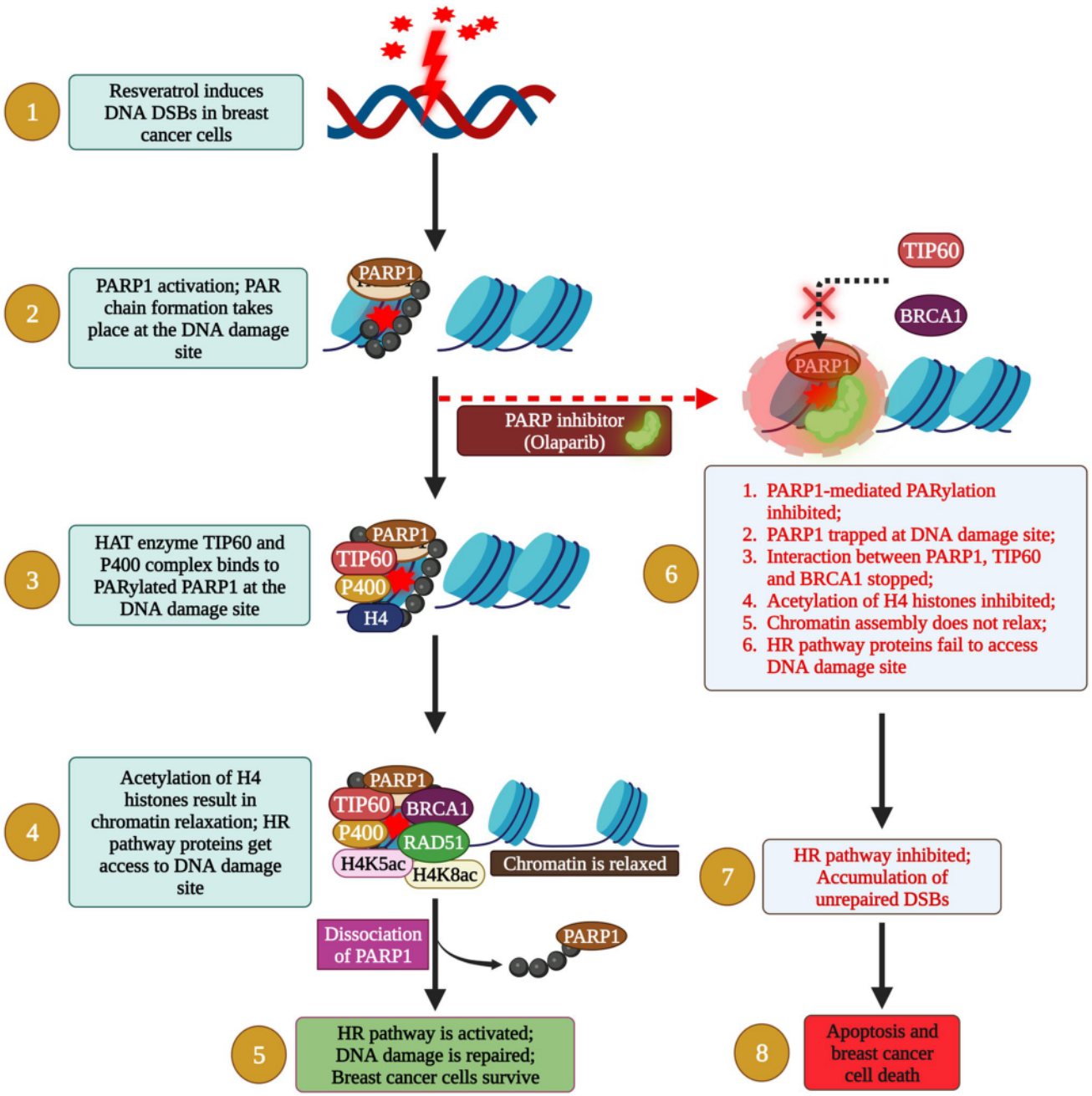

Fig. 6 Schematic representation of the mode of action of RES + OLA combination in breast cancer cells with respect to chromatin remodeling. (1) Resveratrol (RES) exposure causes a DNA double-stranded break (DSB) in breast cancer cells. (2) PARP1 senses the DNA damage and catalyzes the formation of PAR chains at the DNA damage site. (3) HAT enzyme TIP60 interacts with PARylated PARP1 at the DSB site. (4) TIP60, alongwith P400 motor ATPase, catalyzes histone H4 acetylation, resulting in relaxation of chromatin assembly. This allows BRCA1 to interact with PARylated PARP1 and TIP60 at the DSB site. BRCA1, in turn, activates other HR pathway proteins (RPA70, BRCA2, RAD51, etc.). Then, auto-PARylation of PARP-1 takes place, resulting in dissociation of PARP-1 from the HR complex. (5) Activated HR cascade successfully repairs the DSB and the cancer cell survives. (6) When RES-treated breast cancer cells are exposed to OLA, PARP1-mediated PARylation is inhibited and PARP1 is trapped at the DSB site. This causes termination of the PARP1-dependent cooperative interaction between TIP60, and BRCA1. TIP60-mediated acetylation of H4 histones does not take place, thereby stopping chromatin relaxation. As a result, the HR proteins do not get access to the DNA damage site. (7) HR pathway is inhibited, which leads to accumulation of DSBs in the cancer cells. (8) This results in cell cycle arrest, apoptosis, and cancer cell death. (*Created with BioRender.com*)

and the acetylated H4 products, and blocked the physical interaction between TIP60, PAR, and BRCA1, indicating that TIP60 and BRCA1 interaction is dependent on PARP1-mediated PARylation. The combinatorial exposure showed higher PARP1 trapping efficiency in comparison to RES-treated cells. In the DR-GFP plasmid-based HR efficiency assay, addition of OLA in pCBASceI-transfected cells markedly reduced the GFP-positive cell population, clearly indicating that OLA deregulated HR pathway activity (Fig. 5). Taken together, the experimental results revealed that RES + OLA combination treatment inhibited PARP1 activity in the chromatin, and blocked TIP60-mediated chromatin relaxation, which, in turn, affected PARP1-dependent TIP60-BRCA1 association, resulting in deregulation of HR pathway in breast cancer cells.

Finally, in Fig. 6, we have provided a schematic representation of the mode of action of RES + OLA combination in breast cancer cells with respect to chromatin remodeling. (1) Resveratrol (RES) exposure causes a DNA double-stranded break (DSB) in breast cancer cells. (2) PARP1 senses the DNA damage and catalyzes the formation of PAR chains at the DNA damage site. (3) HAT enzyme TIP60 interacts with PARylated PARP1 at the DSB site. (4) TIP60, alongwith P400 motor ATPase, catalyzes histone H4 acetylation, resulting in relaxation of chromatin assembly. This allows BRCA1 to interact with PARylated PARP1 and TIP60 at the DSB site. BRCA1, in turn, activates other HR pathway proteins (RPA70, BRCA2, RAD51, etc.). Then, auto-PARylation of PARP-1 takes place, resulting in dissociation of PARP-1 from the HR complex. (5) Activated HR cascade successfully repairs the DSB and the cancer cell survives. (6) When RES-treated breast cancer cells are exposed to OLA, PARP1-mediated PARylation is inhibited and PARP1 is trapped at the DSB site. This causes termination of the PARP1-mediated cooperative interaction between TIP60, and BRCA1. TIP60-mediated acetylation of H4 histones does not take place, thereby stopping chromatin relaxation. As a result, the HR proteins do not get access to the DNA damage site. (7) HR pathway is inhibited, which leads to accumulation of DSBs in the cancer cells. (8) This results in cell cycle arrest, apoptosis, and cancer cell death.

Conclusion

In summary, the present study conclusively showed that RES + OLA combination efficiently inhibited PARP1-mediated PARylation and trapped PARP1 at the DSB-containing site and simultaneously inhibited the function of TIP60 histone acetylation enzyme, which stopped H4 acetylation. This deregulated the chromatin relaxation process, and in turn, affected the cooperative interaction between PARP1, TIP60 and BRCA1, which resulted in inhibition of the HR pathway in breast cancer cells.

Supplementary Information The online version contains supplementary material available at https://doi.org/10.1007/s12032-023-02279-0.

Acknowledgements The authors would like to sincerely thank the Indian Council of Medical Research (ICMR), Government of India, for providing a research fellowship (Ref. No.: 3/2/2/53/2019/Online Onco Fship/NCD-III) to Saptarshi Sinha and a research grant (Ref. No.: 2016-0043/SCR/ADHOC-BMS) to Chanakya Nath Kundu. We would also like to thank the Acharya Harihar Regional Cancer Centre, Cuttack, Odisha, India for providing us the breast cancer tissue samples from the patients admitted at their facility.

Author contribution SS: Conceptualization, Methodology, Investigation, Validation, Visualization, Writing—original draft, Writing—review and editing. SP: Formal analysis, Validation, Visualization, Methodology. SSA: Validation, Visualization, Methodology, Resources. CD: Visualization, Methodology, Resources. SRD: Visualization, Methodology, Resources. SB: Visualization, Methodology, Resources. RP: Visualization, Methodology, Resources. BD: Methodology, Resources. CNK**:** Project administration, Supervision, Conceptualization, Methodology, Investigation, Validation, Visualization, Writing—review and editing.

Funding This research work was partially supported by Indian Council of Medical Research (Ref. No: 2016-0043/SCR/ADHOC-BMS), Government of India and Kalinga Institute of Industrial Technology (KIIT), Deemed to be University.

Data availability The datasets used and/or analyzed during the current study are available from the corresponding author on reasonable request.

Declarations

Conflict of interest The authors have no competing financial and/or non-financial interests to declare that are relevant to the content of this article.

Ethical approval All the patient tissue samples were used to carry out experiments by following the guidelines of the Declaration of Helsinki after getting the formal approval of the Institutional Ethics Committee (Ethical clearance approval Regd. #ECR/297/Inst/OR/2013) from Acharya Harihar Regional Cancer Centre, Cuttack, Odisha, India.

Consent for publication All authors approve the submission of the manuscript.

References

1. Sung H, Ferlay J, Siegel RL, Laversanne M, Soerjomataram I, Jemal A, et al. Global cancer statistics 2020: GLOBOCAN estimates of incidence and mortality worldwide for 36 cancers in 185 countries. Cancer J Clin. 2021;71:209–49.
2. Ji X, Lu Y, Tian H, Meng X, Wei M, Cho WC. Chemoresistance mechanisms of Breast cancer and their countermeasures. Biomed Pharmacother. 2019;114:108800.

3. Sinha S, Molla S, Kundu CN. PARP1-modulated chromatin remodeling is a new target for cancer treatment. Med Oncol. 2021;38:118.
4. Helleday T. The underlying mechanism for the PARP and BRCA synthetic lethality: clearing up the misunderstandings. Molecular Oncol 2011;5:387–93. Available from: https://www.sciencedirect.com/science/article/pii/S1574789111000743.
5. Jiang W, Murphy JD, Van De Rijn M, Donaldson SS. Secondary breast angiosarcoma and germ line BRCA mutations: discussion of genetic susceptibility. J Radiat Oncol. 2013;2:331–5. Available from: http://link.springer.com/https://doi.org/10.1007/s13566-013-0096-5.
6. Rose M, Burgess JT, O'Byrne K, Richard DJ, Bolderson E. PARP inhibitors: clinical relevance, mechanisms of action and tumor resistance. Front Cell Dev Biol. 2020;8:564601. Available from: https://www.frontiersin.org/articles/https://doi.org/10.3389/fcell.2020.564601/full.
7. De Talhouet S, Peron J, Vuilleumier A, Friedlaender A, Viassolo V, Ayme A, et al. Clinical outcome of Breast cancer in carriers of BRCA1 and BRCA2 mutations according to molecular subtypes. Sci Rep. 2020;10:1–9.
8. Sinha S, Chatterjee S, Paul S, Das B, Dash SR, Das C, et al. Olaparib enhances the resveratrol-mediated apoptosis in Breast cancer cells by inhibiting the homologous recombination repair pathway. Exp Cell Res. 2022;420:113338.
9. Ray Chaudhuri A, Nussenzweig A. The multifaceted roles of PARP1 in DNA repair and chromatin remodelling. Nat Rev Mol Cell Biol. 2017;18:610–21.
10. Chatterjee S, Dhal AK, Paul S, Sinha S, Das B, Dash SR, et al. Combination of talazoparib and olaparib enhanced the curcumin-mediated apoptosis in Oral cancer cells by PARP-1 trapping. J Cancer Res Clin Oncol. 2022;148:3521–35.
11. Donawho CK, Luo Y, Luo Y, Penning TD, Bauch JL, Bouska JJ, et al. ABT-888, an orally active poly (ADP-ribose) polymerase inhibitor that potentiates DNA-damaging agents in preclinical Tumor models. Clin Cancer Res. 2007;13:2728–37.
12. Tentori L, Leonetti C, Scarsella M, d'Amati G, Vergati M, Portarena I, et al. Systemic administration of GPI 15427, a novel poly (ADP-ribose) polymerase-1 inhibitor, increases the antitumor activity of temozolomide against intracranial Melanoma, glioma, Lymphoma. Clin Cancer Res. 2003;9:5370–9.
13. Leone S, Cornetta T, Basso E, Cozzi R. Resveratrol induces DNA double-strand breaks through human topoisomerase II interaction. Cancer Lett. 2010;295:167–72.
14. Price BD, D'Andrea AD. Chromatin remodeling at DNA double-strand breaks. Cell. 2013;152:1344–54.
15. Ikura M, Furuya K, Fukuto A, Matsuda R, Adachi J, Matsuda T, et al. Coordinated regulation of TIP60 and poly (ADP-Ribose) polymerase 1 in damaged-chromatin dynamics. Mol Cell Biol. 2016;36:1595–607.
16. Nair N, Shoaib M, Sørensen CS. Chromatin dynamics in genome stability: roles in suppressing endogenous DNA damage and facilitating DNA repair. Int J Mol Sci. 2017;18:1486.
17. Courilleau C, Chailleux C, Jauneau A, Grimal F, Briois S, Boutet-Robinet E, et al. The chromatin remodeler p400 ATPase facilitates Rad51-mediated repair of DNA double-strand breaks. J Cell Biol. 2012;199:1067–81.
18. Molla S, Chatterjee S, Sethy C, Sinha S, Kundu CN. Olaparib enhances curcumin-mediated apoptosis in Oral cancer cells by inducing PARP trapping through modulation of BER and chromatin assembly. DNA Repair. 2021;105:103157.
19. Chatterjee S, Sinha S, Molla S, Hembram KC, Kundu CN. PARP inhibitor Veliparib (ABT-888) enhances the anti-angiogenic potentiality of Curcumin through deregulation of NECTIN-4 in Oral cancer: role of nitric oxide (NO). Cell Signal. 2021;80:109902.
20. Dash SR, Chatterjee S, Sinha S, Das B, Paul S, Pradhan R, et al. NIR irradiation enhances the apoptotic potentiality of quinacrine-gold hybrid nanoparticles by modulation of HSP-70 in Oral cancer stem cells. Nanomed Nanotechnol Biol Med. 2022;40:102502.
21. Nayak A, Das S, Nayak D, Sethy C, Narayan S, Kundu CN. Nanoquinacrine sensitizes 5-FU-resistant Cervical cancer stem-like cells by down-regulating Nectin-4 via ADAM-17 mediated NOTCH deregulation. Cell Oncol. 2019;42:157–71.
22. Waghmare SG, Samarin AM, Samarin AM, Danielsen M, Møller HS, Policar T, et al. Histone acetylation dynamics during in vivo and in vitro oocyte aging in common carp cyprinus carpio. Int J Mol Sci. 2021;22:6036.
23. Casati L, Pagani F, Maggi R, Ferrucci F, Sibilia V. Food for bone: evidence for a role for delta-tocotrienol in the physiological control of osteoblast migration. Int J Mol Sci. 2020;21:4661.
24. Siddharth S, Das S, Nayak A, Kundu CN. SURVIVIN as a marker for quiescent-breast cancer stem cells—an intermediate, adherent, pre-requisite phase of Breast cancer Metastasis. Clin Exp Metastasis. 2016;33:661–75.
25. Sethy C, Goutam K, Nayak D, Pradhan R, Molla S, Chatterjee S, et al. Clinical significance of a pvrl 4 encoded gene Nectin-4 in Metastasis and angiogenesis for Tumor relapse. J Cancer Res Clin Oncol. 2020;146:245–59.